JOURNAL OF PROPULSION AND POWER
Vol. 23, No. 4, July–August 2007

Hazard Characterization of Uncoated and Coated Aluminium Nanopowder Compositions

Queenie S. M. Kwok,* Chris Badeen,† Kelly Armstrong,† Richard Turcotte,‡ David E.G. Jones,§ and Valéry Y. Gertsman¶
Natural Resources Canada, Canada Centre for Mineral and Energy Technology, Ottawa, Ontario K1A 0G1, Canada

DOI: 10.2514/1.25181

The thermal properties of various uncoated and coated aluminum nanopowders and their effects on the thermal stability, outgassing behavior, and electrostatic discharge sensitiveness of various energetic materials were studied. These aluminum nanopowders had a mean particle size of 20–120 nm. The coated samples had a layer of 7–25% mass of polymer. The thermal behavior of the aluminum nanopowders in air was determined, and the effects of the particle size and the coating on the reactivity of aluminum nanopowders are discussed. Aluminium nanopowders are very reactive in the presence of water, resulting in aging problems. The coating of polymer has a minor effect on the reactivity of aluminum nanopowders with water. On the other hand, the results from an aging study show that the coated aluminum nanopowder is more stable than the uncoated nanopowder in humid atmospheres. The addition of some coated aluminum nanopowders lowers the onset temperatures of cyclotrimethylenetrinitramine, trinitrotoluene, and glycidyl azide polymer by ~20°C. Outgassing results obtained for various cyclotrimethylenetrinitramine/aluminum mixtures at 100°C show that the uncoated Al120 enhances the low-temperature solid-phase decomposition of cyclotrimethylenetrinitramine. The addition of uncoated aluminum nanopowders has previously been shown to increase the electrostatic discharge sensitiveness of both ammonium dinitramide and ammonium perchlorate to ignition energies that can easily be carried by a human body. In contrast, the coated aluminum nanopowders do not appear to sensitize ammonium dinitramide and ammonium perchlorate toward electrostatic discharge, which suggests that the coatings can effectively prevent the sensitization effect.

Nomenclature

A	=	absorbance
A_p	=	differential thermal analysis peak area
d_m	=	mean particle diameter
$R_{\max}$	=	maximum self-heating rate
T_o	=	onset temperature
ΔH	=	enthalpy change
Δm_1	=	first mass gain for early oxidation
Δm_2	=	second mass gain obtained after the melting point of aluminum

Introduction

ALUMINUM powder is commonly added to explosives and propellants compositions to improve their performance, and conventional Al powder is typically micron-sized. Advances in metal processing technology have allowed Al nanopowders to become commercially available**. Because of its large specific surface area, Al nanopowder can produce dramatic improvements in the performance of some energetic materials (EM) [1–4].

On the other hand, the high reactivity of Al nanopowder has also been shown to cause aging problems, particularly in an environment of high relative humidity [5,6]. Subsequent use of the aged material in explosives and propellant compositions would result in significant losses in performance. A coating has been proposed as a solution to protect Al nanopowder from aging, and several coating methods or materials have been investigated [7–11].

The Canadian Explosives Research Laboratory (CERL) has published thermal and sensitiveness results for uncoated Al nanopowders and their mixtures with various EM [5,12–15]. To further investigate the effect of particle size and coating on the reactivity of Al nanopowders, the thermal properties of various coated and uncoated Al nanopowders were studied. The present paper also compares the effect of coated and uncoated Al nanopowders on the thermal stability, outgassing behavior, and electrostatic discharge (ESD) sensitiveness of various EM.

Experimental

Materials

Eleven samples of Al nanopowders of different particle sizes and with various coatings were used in this study. The manufacturing process, the d_m provided by the manufacturers, and the nature of the coatings for these Al nanopowders are summarized in Table 1. The thicknesses or percentages of coating quoted in Table 1 were provided by the manufacturers and were not verified. The bare Al nanopowders were produced by Nanotechnologies Inc.†† Al nanopowders were coated with polyethylene (PE) and polypropylene (PP) using the Ziegler–Natta process [16]. To prevent aging of the samples, all of the Al nanopowder samples were stored in desiccators filled with argon.

Trinitrotoluene (TNT), glycidyl azide polymer (GAP), ammonium dinitramide (ADN), and ammonium perchlorate (AP) were obtained from Defence Research and Development Canada—Valcartier. Cyclotrimethylenetrinitramine (RDX) produced by

Received 15 May 2006; revision received 13 April 2007; accepted for publication 13 April 2007.

*Thermal Hazard Scientist, Canadian Explosives Research Laboratory, 555 Booth Street; qkwok@nrcan.gc.ca.
†Thermal Hazard Scientist, Canadian Explosives Research Laboratory, 555 Booth Street.
‡Explosives Research and Development Section Head, Canadian Explosives Research Laboratory, 555 Booth Street.
§Emeritus Scientist, Canadian Explosives Research Laboratory, 555 Booth Street.
¶Research Scientist, Materials Technology Laboratory, 568 Booth Street.

**Data available online at www.argonide.com and www.nanoscale.com.
††Data available online at www.nanoscale.com.

Table 1 Characteristics of Al nanopowders

Name	Process	d_m, nm[a]	Al content, %[a]	Coating[a]
Al-T20	Gas condensation	17	35	2 nm Al_2O_3
Al-T50	Gas condensation	48	69	2 nm Al_2O_3
Al-T80	Gas condensation	84	82	2 nm Al_2O_3
Al-N50	Plasma evaporation	52	——	1 nm Al_2O_3
Al-N80	Plasma evaporation	85	80	1.7 nm Al_2O_3
Al120	Gas condensation	120	——	4.2 nm Al_2O_3
Al120PE7	Gas condensation	120	——	7% PE
Al120PE19	Gas condensation	120	——	19% PE
Al120PE10	Gas condensation	120	——	10% PE
Al120PE25	Gas condensation	120	——	25% PE
Al120PP	Gas condensation	120	——	10% PP

[a]Values provided by the manufacturers; d_m and thicknesses were measured by manufacturers using BET.

Expro Technologies, Inc. was used in this work. Except for GAP, all of the samples were used as received. GAP was shipped as a 20% solution in 1,2-dichloroethane, and GAP samples were dried in a desiccator under vacuum.

Various mixtures of RDX/Al, TNT/Al, GAP/Al, ADN/Al, AP/Al, and Al/H_2O were prepared at CERL for the thermal stability, aging, outgassing, and ESD sensitiveness studies. For the aging studies, aged samples were prepared by placing them in a bell jar at a relative humidity greater than 80% at room temperature.

Differential Scanning Calorimetry

A TA Instruments 2910 differential scanning calorimetry (DSC) module was used for the thermal studies of Al nanopowders in air. Al pans containing 2.0 mg of Al nanopowders were heated from 30 to 600°C at 1°C min^{-1}. The DSC was calibrated for heat flow [17] and temperature [18].

Thermogravimetry and Differential Thermal Analysis

A TA Instruments 2960 Simultaneous thermogravimetry and differential thermal analysis (TG-DTA) was also used for assessing the thermal behavior of Al nanopowders in air (50 cm^3 min^{-1}). Equal amounts (~10 mg) of sample and reference material (platinum) were placed in alumina pans and heated at 20°C min^{-1} from 30 to 1200°C. TG mass, DTA baseline, and temperature calibrations [18] were performed before the experiments.

Evolved Gas Analysis During TG-DTA

The TG-DTA was also interfaced to a Bomem MB100 Fourier transform infrared spectrometer (FTIR) and a Balzers Thermostar GSD300 Quadrupole mass spectrometer (MS) for the outgassing experiments. Samples and reference (platinum) of 20 mg were heated at 5°C min^{-1} to 100°C, and then held isothermally for 40 min in helium (100 cm^3 min^{-1}). The acquisition rate of the FTIR was two scans every minute. MS data were acquired using a bar graph scan, from 5 to 100 amu at a speed of 0.2 s amu^{-1}.

Accelerating Rate Calorimetry

The thermal stability of the samples was studied using accelerating rate calorimetry (ARC). Calorimeters distributed by TIAX LLC and Thermal Hazard Technology were used. Samples of 0.3–1.1 g were placed in lightweight spherical titanium vessels. The experiments on Al nanopowders were started at ambient pressure and at 1.4 MPa of air. The experiments in wet environments were performed in air and argon using a 10:1 mixture of Al nanopowders and water. For RDX, TNT, GAP, and their mixtures with Al nanopowders, the experiments were started at ambient pressure of air (RDX and TNT) or argon (GAP). The standard ARC procedure of "heat-wait-search" was used [19].

Particle Characterization

For the particle characterization, Al120, Al120PE7, and Al120PE19 were examined using a Philips CM20 FEG transmission electron microscope (TEM). Chemical microanalysis was performed using an Oxford Instruments thin-window energy-dispersive spectrometry (EDS) detector with an INCA system analyzer. More details of TEM techniques are given elsewhere [14].

ESD Apparatus

ESD sensitiveness of the ADN/Al (75:25) and AP/Al (80:20) mixtures were determined using an ESD apparatus manufactured by Franklin Applied Physics. The apparatus is described elsewhere [20]. The ESD tests were performed with both open and closed sample containers. For the open containers, the tip of the pin electrode was positioned 0.5 mm above the mixture. For the closed containers, the top of the container was sealed with a piece of plastic tape and the pin electrode was lowered until it just pierced the tape. The minimum ignition energy was determined by subjecting the sample to sparks of varying energies. A positive reaction was defined when the sample burned completely. The highest energy delivered by the apparatus was 156 mJ, which is a factor of 10 higher than the most commonly accepted maximum energy value that a human body can deliver [21].

Results and Discussion

Thermal Properties of Al Nanopowders

Thermal Behavior of Al Nanopowders in Air

DSC and TG-DTA Results. The DSC and TG-DTA results for the various Al nanopowders in air are shown in Figs. 1–3. The various Al nanopowders exhibit an exothermic peak and a mass gain between ~400°C and the melting point of Al (~660°C). This exotherm and mass gain observed in air have been shown to result from an oxidation of solid Al nanopowders [5]. The onset temperature, the enthalpy change, the peak area, and the mass gain obtained for this early oxidation of the various Al nanopowders are summarized in Table 2.

Except for Al-T80 and Al120PE7, the exotherms and mass gains observed from the TG-DTA results for most of the Al nanopowders are considered to be thermal runaway resulting from oxidations of Al

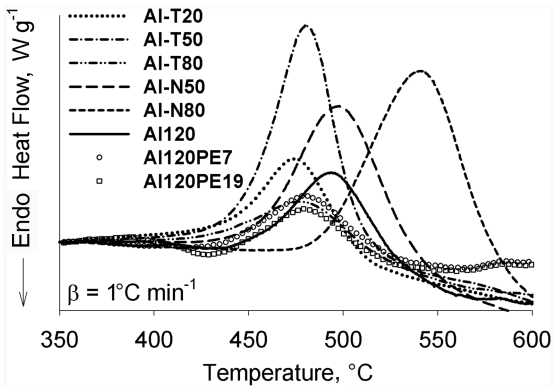

Fig. 1 Comparison of DSC results for Al nanopowders in air.

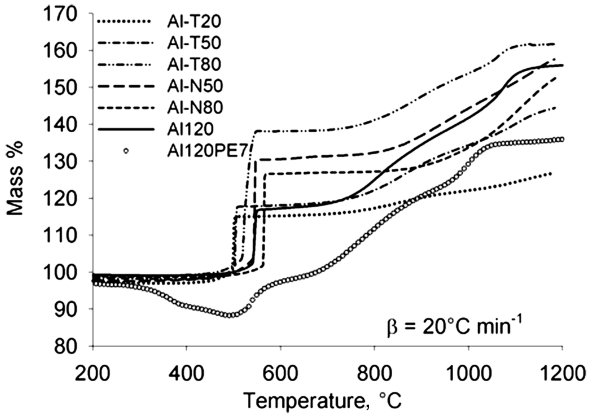

Fig. 2 Comparison of TG results for Al nanopowders in air.

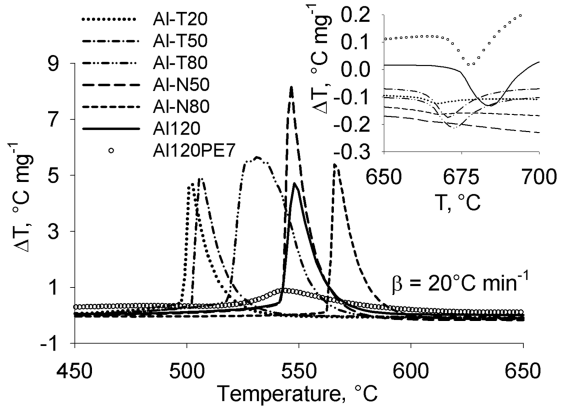

Fig. 3 Comparison of DTA results for Al nanopowders in air.

nanopowder, as described by Johnson et al. [22]. No thermal runaway was observed from the DSC results, because a slower heating rate was used in the DSC study (1°C min^{-1}) than that used in the TG-DTA study (20°C min^{-1}). The runaway reaction caused the incomplete oxidation of Al. As shown in Table 2 and Fig. 2, the mass gains obtained from the various uncoated Al nanopowders between 400 and 600°C were between 18–39%. The expected mass gain for the complete oxidation of Al is 89%. If the 18–39% mass gain only resulted from oxidation, the TG-DTA results imply that less than 44% of the Al nanopowder is oxidized to Al_2O_3 below the melting point of Al. The remainder of the sample corresponds to the unreacted Al and to the passivating layers in the original samples.

The melting endotherm of Al near 660°C observed for most of the Al nanopowders (Fig. 3, inset) indicates that an unreacted Al core remained in these Al nanopowders after the early incomplete oxidation. No significant melting endotherm was observed for Al-N50 and Al-N80; nearly complete conversion to Al oxide and nitride may have occurred in the thermal runaway of these two samples. A second mass gain was also observed for the various Al nanopowders in air above the melting point of Al (Fig. 2). This mass gain may be due to a second stage of oxidation and/or a nitridation of the unreacted Al core. The second mass gain obtained for the various Al nanopowders is also summarized in Table 2.

Al-T20, Al-T50, and Al-T80 have a similar thickness of passivating layer (2 nm), whereas their mean particle sizes are different. The TG-DTA results show that the onset temperature, the peak area, and the mass gain for the oxidation of these three samples decrease as the particle size decreases. The smallest Al nanopowder (Al-T20) is most reactive in air in terms of the onset temperature; however, it has a lower mass gain and a smaller exotherm than Al-T50 and Al-T80. The low mass gain and small exotherm observed for Al-T20 may result from its relatively lower content of Al, because it has the same thickness of passivating layer as the larger Al nanopowders (Al-T50 and Al-T80).

The DSC results also show that the onset temperature for the oxidation of the three Al-T samples decreases as the particle size decreases. However, the DSC results do not totally agree with the TG-DTA results. In the DSC results, the largest exotherm among these three samples was observed for Al-T50, instead of Al-T80 as observed from the TG-DTA results. These differences may result from the different experimental conditions used. The TG-DTA experiments for ~10 mg of sample contained in an open pan with a surface area of 23 mm^2 were performed at 20°C min^{-1}, whereas the DSC experiments were carried out at 1°C min^{-1}, using ~2 mg of sample and an open pan with a surface area of 30 mm^2.

Particle size had a similar effect on the onset temperatures for Al-N50 and Al-N80 to that observed for the Al-T samples. Al-N50 and Al-N80 have a mean particle size of 52 and 85 nm, respectively, and Al-N50 has an onset temperature that is about 40°C lower than Al-N80 (Table 2).

The effect of the thickness of the passivating layer was studied by comparing Al nanopowders of similar mean particle size. Al-N50 and Al-T50 have passivating layers of 1 and 2 nm, respectively. The oxidation of Al-N50 has a higher onset temperature than that for Al-T50 (Table 2), even though the Al nanopowder with a thinner passivating layer is expected to be more reactive than the Al nanopowder with a thicker oxide layer. However, the TG-DTA and DSC results indicate that the difference of 1 nm in the thickness of

Table 2 Comparison of DSC and TG-DTA results for Al nanopowders

	DSC		TG-DTA			
Sample	T_o, °C[a]	ΔH, kJ g^{-1}	T_o, °C[a]	A_p, °C min mg^{-1}[b]	Δm_1, %[c]	Δm_2, %[d]
Al-T20	353	5.7	403	3.5	18	12
Al-T50	363	10.3	410	3.6	20	27
Al-T80	389	3.6	417	8.5	39	23
Al-N50	421	8.6	442	8.3	33	27
Al-N80	462	10.3	487	3.4	28	26
Al120	438	4.5	368	3.8	18	39
Al120PE7	420	2.8 (3.0)[e]	479	1.3	11[f]	42[f]
Al120PE19	431	2.3 (2.8)[e]	—	—	—	—
Alex [12]	460	3.9	466	3.3	17	37
Als [5]	399	5.5	406	3.5	21	26
Alss [13]	~390[g]	1.6	~430[g]	1.8	12	5
Alsstef [13]	~380[g]	2.6	~532[g]	2.4	11	0.7

[a]Temperature at which a deflection from the established baseline is observed.
[b]May be correlated with ΔH and can be used for qualitative comparison.
[c]Mass gain obtained between ~400 and 600°C.
[d]Mass gain obtained after the melting point of Al.
[e]Values in parentheses represent the ΔH per gram of uncoated Al powder.
[f]Values of mass percent are calculated using the mass of uncoated Al powder, that is, initial mass—mass loss (12%).
[g]Overlapped with other exotherm.

passivating layer may not necessarily be the only factor determining the reactivity of Al nanopowders of similar mean particle size. As stated in Table 1, Al-N50 and Al-T50 were produced by different processes. The reactivity of Al nanopowders may also be affected by the particle size distribution, agglomeration of powders, specific surface area, and composition of the passivating layer.

As compared in Table 2, the enthalpy change obtained for the early oxidation of coated and uncoated Al120 decreases as the mass percent of PE coating increases. The TG-DTA results also show that Al120PE7 has a lower peak area and a lower mass gain than Al120. Therefore, the addition of PE coating appears to lower the reactivity of solid Al nanopowders with air.

Two mass losses were observed for Al120PE7 below 480°C. The first mass loss (3%) was observed below 230°C and was accompanied by a minor endotherm. These mass losses and endotherms resulted from outgassing of the sample, and this is further discussed later in this paper. The second mass loss observed between 230 and 480°C was 8%. Because this mass loss was also accompanied by an exotherm, it was most likely due to the decomposition of the coating material. This 8% mass loss corresponds approximately to the expected amount of PE coating (7%).

The results for the various Al nanopowders are compared with the earlier results obtained for Alex [12], Als [5], Alss [13], and Alsstef [13] in Table 2. Alex and Als have a mean particle size of 180 and 90 nm, respectively. The particle size of Alss is in the range of 20–50 nm, and Alsstef is Alss coated with ~18% mass fluoropolymer.

The 12 Al nanopowders, which have differences in particle sizes and passivating layers, showed significant differences in onset temperature, enthalpy change, and mass gain on oxidation. Among the 12 different Al nanopowders, the oxidation of the smallest (Al-T20) has the lowest onset temperature (Table 2). On the other hand, Al-N80 (which has a smaller mean particle size than Al120, Alex, and Als) has the same onset temperature as Alex. The TG-DTA and DSC results suggest that the mean particle size and the thickness of the oxide layer affect the reactivity of Al nanopowder to some extent. Some other factors, such as particle size distribution, agglomeration of powders, specific surface area, and composition of the passivating layer may also affect the reactivity of Al nanopowders.

ARC Results. The thermal behavior of the various Al nanopowders in air was also studied using ARC. The ARC results for the various Al nanopowders are summarized in Table 3. In ARC experiments with initial ambient pressure of air, minor exotherms (which had self-heating rates between 0.02–0.03°C min^{-1}) were observed for Al-T20, Al-T50, and Al-T80, starting at 185, 190, and 195°C, respectively. The onset temperatures for the oxidation of these Al nanopowders appear to decrease as their mean particle sizes decrease. The oxidation of Al-N50 has an onset temperature of 85°C, whereas no exotherm was observed up to 260°C for Al-N80, Al120, and Al120PE19.

Mass losses were observed for the seven Al nanopowders in ambient air (Table 3). These mass losses suggest the occurrence of an outgassing. The outgassing behavior of Al nanopowders was studied using different techniques and is further discussed later in this paper.

In ARC experiments starting at 1.4 MPa of air, oxidation of Al-T20, Al-T50, Al-T80, and Al-N80 gives a lower onset temperature than observed for ambient air (Table 3). These exotherms also display higher R_{max} than those in ambient air. Among the five samples studied, the smallest Al nanopowder (Al-T20) exhibited the lowest onset temperature and the largest exotherm for the oxidation at superambient pressure of air. The ARC results suggest that the mean particle size affects the reactivity of Al nanopowder in air.

Reactivity with Water

ARC was also used to investigate the thermal stability of the Al nanopowders in a wet environment. The ARC results for the 10:1 mixtures of Al nanopowders and water are shown in Table 3. Except for Al-T20/H_2O in argon, exotherms were detected for all of the mixtures of Al nanopowders and water in air or in argon at an onset temperature of just 30 to 40°C (Table 3). The exotherm observed in argon for Al-T20/H_2O has an onset temperature of 73°C. The ARC results show that Al nanopowders are very reactive with water.

For most of the mixtures of Al nanopowder and water, the exotherms in air and in argon have similar onset temperatures. These exotherms started at temperatures less than 40°C and result from a reaction between Al and water. Additionally, there may be a contribution of oxygen to this reaction process such as $2Al + 1.5O_2 + H_2O = 2AlOOH$, because the exotherms in air have higher R_{max}. Generally, the presence of oxygen is not required to initiate the reaction between Al and water at elevated pressure, because the exotherms observed in air and in argon have similar onset temperatures.

Table 3 Comparison of ARC results for various Al nanopowders

Sample	Initial P, MPa	P_r, MPa[a]	Mass, g	Δm, %	T_o, °C[b]	R_{max}, °C min^{-1}
Al-T20	0.11 (air)	0.14	1.1	−2.7	185	0.025
	1.4 (air)	1.4	1.0	2.6	113	0.18
Al-T20/H_2O	1.4 (air)	1.3	1.0	2.1	41	>5
	1.4 (Ar)	1.7	1.0	−0.3	73	0.048
Al-T50	0.11 (air)	0.15	1.0	−0.4	190	0.030
	1.4 (air)	1.2	1.0	2.8	147	0.059
Al-T50/H_2O	1.4 (air)	0.11	1.1	7.2	30	>5
	1.4 (Ar)	1.7	1.0	−0.2	39	0.055
Al-T80	0.11 (air)	0.11	1.0	−0.1	195	0.020
	1.4 (air)	1.2	1.1	2.5	139	0.030
Al-T80/H_2O	1.4 (air)	1.1	1.0	1.9	31	>5
	1.4 (Ar)	1.9	1.0	−0.4	30	1.0
Al-N50	0.11 (air)	0.21	0.6	−1.0	85	0.21
	1.4 (air)	0.59	0.5	5.0	121	0.082
Al-N50/H_2O	0.11 (air)	0.44	0.5	−1.6	34	0.080
	1.4 (Ar)	1.6	0.5	−0.4	37	0.059
Al-N80	0.11 (air)	0.14	0.5	−0.9	——[c]	——
	1.4 (air)	1.0	0.6	2.9	183	0.025
Al-N80/H_2O	1.4 (air)	1.4	0.5	2.6	38	1.6
	1.4 (Ar)	2.0	0.9	−0.6	35	0.039
Al120PE7	0.11 (air)	0.26	1.1	−0.5	——[c]	——
Al120PE7/H_2O	0.11 (air)	0.40	1.1	−0.4	32	>1
Al120PE19	0.11 (air)	0.10	1.0	−0.3	——[c]	——
Al120PE19/H_2O	0.11 (air)	0.38	1.0	−0.5	33	>1

[a]Pressure recorded after the system was allowed to cool to ~30°C.
[b]Onset temperature for the first detected exotherm.
[c]No exotherm observed below 260°C.

The onset temperature obtained for the Al-N50/H_2O mixture in ambient air is similar to that for the other Al nanopowders at 1.4 MPa of air (Table 3), which suggests that the pressure of air has little effect on the onset temperature. However, the lower R_{max} observed for Al-N50/H_2O compared with the rates observed for the other Al nanopowders at 1.4 MPa of air suggests that Al nanopowder is relatively less reactive with water at ambient air pressure.

For the five Al nanopowders tested in argon (Table 3), the exotherm of Al-T20/H_2O displays the highest onset temperature at elevated pressure. The ARC results suggest that Al-T20 is least reactive with water in an inert environment. Although Al-T20 has the smallest mean particle size, the sample may comprise agglomerates of the fine particles, which may be less reactive with water. The reactivity of Al nanopowders with water may cause aging of Al nanopowder, as discussed in [5].

An exotherm was also detected for Al120PE19/H_2O in air at an onset temperature of about 30°C, which is similar to that for Al120/H_2O. Both experiments were stopped automatically at about 50°C, when the self-heating rates exceeded the automatic termination threshold (1°C min^{-1}). The low onset temperatures and the runaway reactions observed from the mixtures show that the coated Al nanopowder is still very reactive with water. The coating of PE was added to the Al nanopowders in an attempt to improve the thermal stability of Al nanopowders in air and in wet environments. However, the ARC results show that the PE coating is not effective in reducing the reactivity of Al nanopowder with water. This result may derive from the nonuniform coverage of the coating on the surface of Al nanopowders, which was observed from a TEM-EDS analysis. The TEM-EDS results for the Al nanopowders are discussed later in this paper.

Aging Behavior

Al nanopowder has been shown to react with water that was adsorbed on the samples during an exposure to a wet environment [5,6]. The reactivity of Al nanopowder with adsorbed water has been shown to produce Al_2O_3 or $Al(OH)_3$ and to cause aging of Al nanopowder [5,6]. Earlier DSC results have demonstrated that the reactivity of Al nanopowder in air depends on the aging conditions of the material [12].

To further study the aging of Al nanopowder, aged samples of Al120 and Al120PE7 were prepared by exposing them to an environment with a relative humidity greater than 85% at room temperature. To determine the extent of reaction with moisture, TG-DTA experiments were conducted every week on the aged samples in air to determine their reactivity and Al content.

As shown in Fig. 4a, a decrease in mass gain and exotherm peak area was observed when Al120 had been exposed to the humid atmosphere for 28 days. This decrease in mass gain and peak area, as well as the presence of white and light gray powders in the aged Al120 before the TG-DTA experiments, suggest that Al_2O_3 or $Al(OH)_3$ was formed from exposure to moisture. Al120 was almost completely reacted in 49 days [i.e., no further mass gain in the TG study (Fig. 4a)].

It can also be observed from Fig. 4a that the aged Al120 shows a substantial mass loss at temperatures below 300°C. This mass loss was due to desorption of the water adsorbed on the surface of the aged samples. The amount of adsorbed water and the aging of Al120 increase as the time of exposure to humid atmosphere increases. The adsorbed water on the surface of the Al nanopowder enhances the aging reaction of Al nanopowders.

For Al120PE7, the aged samples exhibit a higher reactivity (i.e., a higher peak area and mass gain) in air than the fresh sample (Fig. 4b) below the melting point of Al. The two aged samples of Al120PE7 exhibited the thermal runaway, whereas the fresh sample showed a controlled oxidation. The aged samples of Al120PE7 also have a higher mass loss than the fresh sample, whereas the total mass gains obtained from the fresh and aged samples are consistent. The results suggest that more water was adsorbed on the surface of the aged samples, and the adsorbed water did not react with and further age the Al nanopowders. Moreover, the adsorbed water may disrupt the PE coating and allows the Al to react with air. The results show that the PE coating significantly decreases the aging of the Al nanopowder in a moist environment.

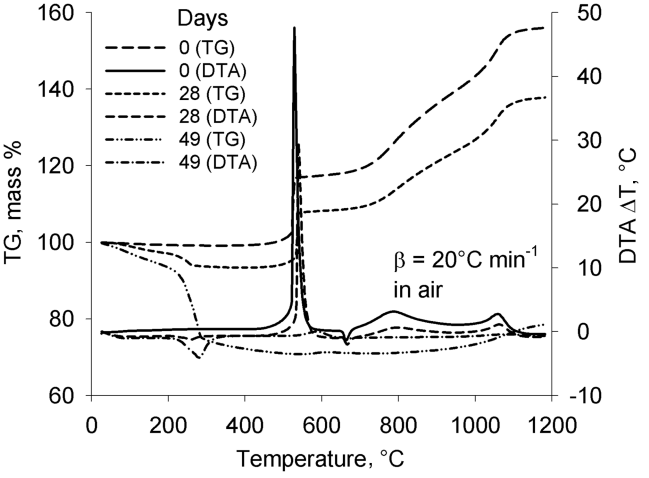

a)

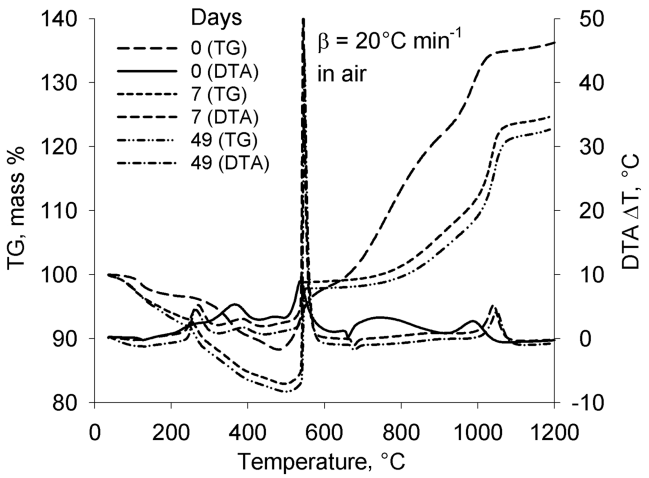

b)

Fig. 4 TG-DTA results for aging studies of a) Al120, b) Al120PE7.

Outgassing Studies

Earlier outgassing studies have shown the presence of adsorbed water and carbon dioxide on the surface of various Al nanopowders [13]. The adsorption of H_2O and CO_2 on Al nanopowders is also particle-size-dependent, with more being adsorbed as the particle size decreases [13]. Water adsorption and desorption is a particular concern in the aging study of Al nanopowders, because the aging reaction of Al nanopowders may be related to the water adsorbed on its surface. Therefore, it is of interest to study the outgassing behavior of Al nanopowders.

The outgassing behavior of Al120, Al120PE7, and Al120PE19 at an isothermal temperature of 100°C was studied using TG-DTA-FTIR-MS. Example plots using Al120PE19 are shown in Fig. 5. The TG and temperature curves were plotted against time in Fig. 5a. The absorbance versus time for the evolved gases detected by FTIR is shown in Fig. 5b, and the MS data are presented as ion current versus time for selected mass fragments in Fig. 5c. The TG-DTA-FTIR-MS results obtained for the coated and uncoated Al120 are summarized in Table 4. The uncertainties for the TG mass losses in Table 4 represent the mass loss percent due to the baseline drift of the TG signals ($\sim$10 μg).

Mass losses and desorptions of H_2O and CO_2 were obtained for Al120, Al120PE7, and Al120PE19 at 100°C. HNO_3 and HCl were also detected from the two PE-coated samples. These Al

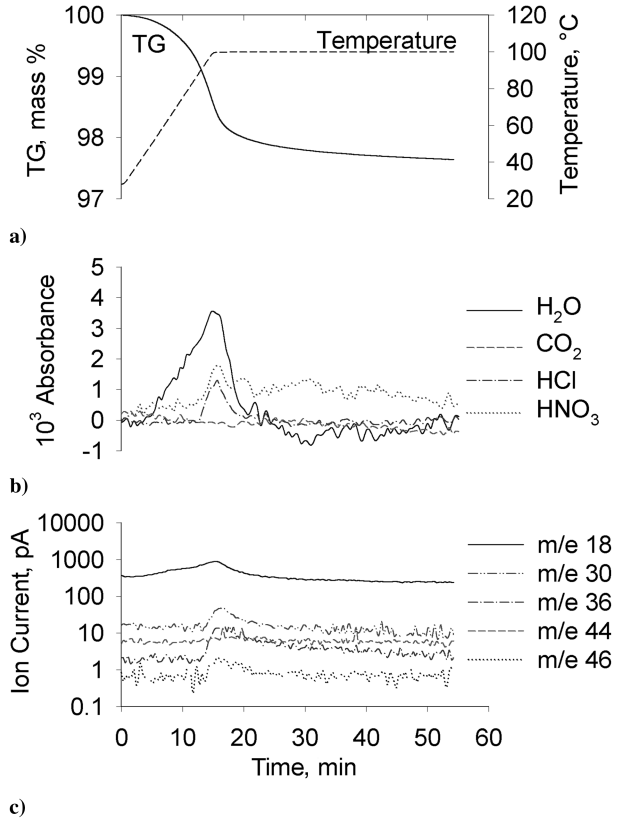

Fig. 5 Results for Al120PE19 in helium for a) TG; b) FTIR; c) MS.

nanopowders were coated with 7–19% of PE by a Ziegler–Natta polymerization reaction [16]. HCl results from the hydrolysis of the cocatalyst of the polymerization ($TiCl_4$) with OH sites on the Al particles. The presence of Ti and Cl in the samples was confirmed by the EDS analysis, as discussed later in the next section. The source of HNO_3 has not yet been identified. Al120PE7 and Al120PE19 have a higher mass loss and higher maximum FTIR absorbances for H_2O and CO_2. The PE-coated samples of Al120 seem to evolve more H_2O and CO_2 than the uncoated sample. Because the full aging history of these coated Al nanopowders are unknown, the higher evolution of H_2O and CO_2 may be due to more exposure to moist environment. These gases may also result from the oxidation of the coating material.

Particle Characterization

The TEM results for Al120, Al120PE7, and Al120PE19 are shown in Fig. 6. Most Al nanopowder particles are single spheres and are agglomerated in loosely assembled clusters. These particles contact each other through outer oxide layers, which indicate that the clustering occurred after the oxidation of metallic cores. On the other hand, longer chains of particles bonded tightly through their metallic

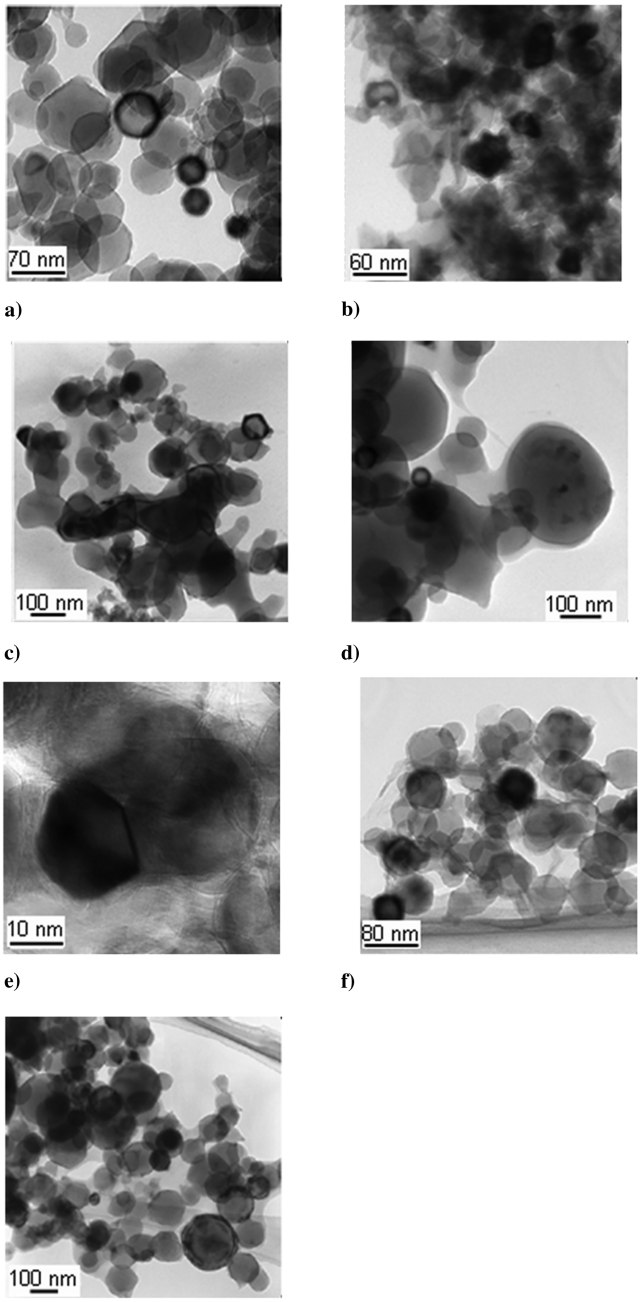

Fig. 6 TEM results for a) Al120, b–e) Al120PE7, and f–g) Al120PE19.

Table 4 Summary of TG-FTIR-MS outgassing results

Sample	Mass, mg	$-\Delta m$ %[a]	FTIR results	10^5 [H_2O], A mg^{-1}	10^5 [N_2O], A mg^{-1} RDX	MS results[b]
Al120	20	0.46 ± 0.07	H_2O, CO_2	5.1	——[c]	m/z 18
Al120PE7	20	2.73 ± 0.07	H_2O, HNO_3, HCl, CO_2	21	——[c]	m/z 18, 30, 36, 46, 44
Al120PE19	18	2.41 ± 0.08	H_2O, HNO_3, HCl, CO_2	20	——[c]	m/z 18, 30, 36, 46
RDX	20	0.22 ± 0.07	H_2O, N_2O	2.0	1.1	m/z 44
RDX/Al120	20	0.56 ± 0.07	N_2O, H_2O, NO_2	2.4	12	m/z 18, 30, 44
RDX/Al120PE10	20	0.76 ± 0.07	H_2O, N_2O	7.2	3.0	m/z 18, 44
RDX/Al120PE25	20	0.63 ± 0.07	H_2O, N_2O	5.4	2.4	m/z 18, 44
RDX/Al120PP	20	0.42 ± 0.07	H_2O, [CH], N_2O	3.8	2.2	m/z 57, 18, 44

[a]Value represents the average mass loss obtained from duplicates; the uncertainty of the value represents the TG baseline drift; and the standard deviation obtained from the repeated measurements is less than the uncertainty of the baseline drift.
[b]Identification of fragments: m/z 18 = H_2O; m/z 30 = NO^+; m/z 36 = HCl; m/z 44 = CO_2, N_2O; m/z 46 = NO_2^+; and m/z 57 = C_xH_y.
[c]Not detected.

Table 5 Summary of TEM and EDS results for Al nanopowders

Sample	Diameter, nm	Thickness of oxide layer, nm	EDS results
Al120	59 ± 22	4.2 ± 0.8	Al, O, Ar, Ta/Si
Al120PE7	68 ± 39	3.8 ± 0.9	Al, O, C, Ti, Ar, Ta/Si, Cl
Al120PE19	73 ± 30	4.0 ± 0.8	Al, O, C, Ti, Ta/Si, Cl, Ar, Na

cores are also observed from the samples (Fig. 6b). There are also some irregularly shaped particles (Fig. 6b), and these irregular shapes may mainly result from a multicrystalline metallic core, as shown by the example in Fig. 6e.

The polymer in Al120PE7 and Al120PE19 is present mostly as chunks or flakes, rather than as a layer around individual particles (Figs. 6b and 6f). Many particles are embedded inside the polymer, which apparently keeps particle clusters together. Some loose particles, which are not firmly attached to the bigger clusters, are also observed from the samples. A thin coating of polymer surrounding individual particles is observed only in a few cases, (Figs. 6d and 6g). As shown earlier by the ARC results for the Al120PE19/H_2O, the nonuniform coverage of the coating causes the ineffectiveness of the coating in preventing a reaction with water.

The particle sizes of the three Al120 samples were estimated by direct measurements of 200–400 particles on the TEM bright-field images. The mean values and the standard deviations obtained are summarized in Table 5. There are insignificant differences in the mean diameters obtained for the three samples, and the average value is 68 ± 33 nm. This value is smaller than that provided by the manufacturer (120 nm), which was determined using the Brunauer–Emmett–Teller (BET) technique.. Surface-absorption techniques such as BET have been shown to give particle sizes significantly different from those measured directly by TEM [14].

The thickness of the passivating alumina layer of the three Al nanopowders was also estimated using the TEM bright-field images of the particles. The mean values, which were obtained from measurements of about 20–30 particles, are summarized in Table 5. The values obtained for the three samples are also consistent, and an average value of 4.0 ± 0.8 nm was obtained. The TEM results are comparable to those obtained from other studies [14,23].

The EDS chemical microanalysis results obtained for the three Al120 samples are shown in Fig. 7 and Table 5. Oxide layers around the particles were observed from the EDS maps for all of the samples (Fig. 7). A chain of particles, which were joined together by their metallic cores and had a common outer oxide layer, was also observed in Fig. 7a. This chain can easily be distinguished from other particles, which simply touch each other or overlap without intergrowth (in the right corner of Fig. 7a). The nonuniform distribution of the polymer in the coated samples was proved by the nonuniform distribution of carbon, as shown in Fig. 7b. Some Al120PE7 and Al120PE19, which were not embedded inside the polymer, were also observed (Figs. 7c and 7d).

In addition to Al, O, and C, EDS spectra also reveal the presence of some impurities in the samples (Table 5). Trace amounts of Ar and Ta (or Si) were detected from all of the samples. Ar is probably an impurity from the manufacturing process, because it was used as a purge gas in the nanopowder manufacturing process [23]. The EDS spectrum identified as Ta can also result from Si. However, in both cases, the source of Ta or Si is not known. Substantial amounts of Ti and Cl were also observed for Al120PE7 and Al120PE19 (Table 5). As discussed earlier in the outgassing result, Ti and Cl come from residual $TiCl_4$, which was used as a cocatalyst in the polymerization reaction [16].

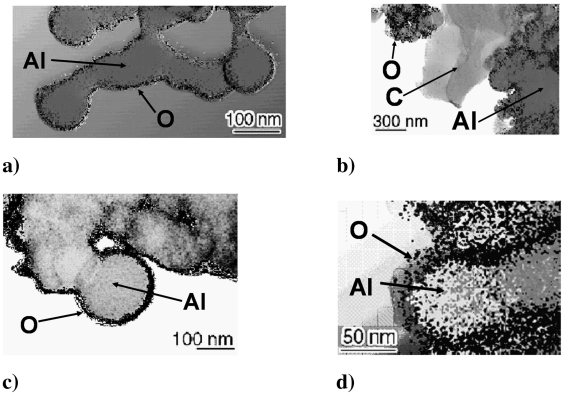

Fig. 7 EDS maps for a) Al120, b–c) Al120PE7, and d) Al120PE19.

ESD Sensitivities

The ESD sensitivities of the various coated and uncoated Al nanopowders are summarized in Table 6. The results show that all of the Al nanopowders have ESD-limiting energies higher than 156 mJ in closed containers.

Al120 ignited at a discharge energy of just 6 mJ when it was placed in an open sample container. Therefore, in this configuration, it could be easily initiated by a discharge from an ungrounded operator. Compared with the coated samples, uncoated Al120 is more sensitive to ESD. Al120PE7 and Al120PE19 have ESD-limiting energies of 25 mJ and greater than 156 mJ, respectively, in open configuration. The ESD sensitivity of Al120 decreases as the amount of coating increases. The particle characterization studies have shown that the Al nanopowders in the coated samples agglomerate and are embedded inside the polymer as clusters. Compared with the uncoated Al nanopowders, these clusters have a smaller surface area, which may decrease the interaction of coated Al nanopowders with the oxygen in air. Therefore, to handle PE-coated Al120 nanopowders, no special precautions to avoid electrostatic charge accumulation on individuals are required.

Effect of Al Nanopowders on EM

Thermal Stability

The thermal stability of RDX, TNT, GAP and their mixtures with Al nanopowders was studied using ARC, and the results are summarized in Table 7 and Figs. 8–10.

The onset temperatures obtained for RDX and its 80:20 mixtures with Al120, Al120PE10, and Al120PE25 are all about 184°C

Table 6 Summary of ESD sensitiveness results

	ESD ignition energy, mJ	
Sample	Closed	Open
Al120	>156	6
Al120PE7	>156	25
Al120PE19	>156	>156
ADN [13]	>156	>156
ADN/Al120 (75:25)	6	6
ADN/Al120PE10	>156	>156
ADN/Al120PE25	>156	>156
ADN/Al120PP	>156	>156
ADN/Alex [13]	>156	>156
ADN/Als [13]	6	6
ADN/Alss [13]	56	25
ADN/Alsstef [13]	>156	>156
AP [5]	>156	>156
AP/Al120 (80:20)	6	6
AP/Al120PE10	>156	>156
AP/Al120PE25	>156	>156
AP/Al120PP	>156	>156
AP/Alex [5]	100	——
AP/Als [5]	6	6

Table 7 Summary of ARC results for EM/Al mixtures

Sample	M, g	T_o, °C[a]	P_r, MPa[b]	E, kJ mol^{-1}	$\ln(Z/\text{min}^{-1})$	$\ln(k/\text{min}^{-1})$
RDX	0.3	184 ± 5	0.30	639 ± 6	164 ± 2	−6 ± 3[d]
RDX/Al120 (80:20)	0.5	182 ± 5	0.30	501 ± 4	129 ± 1	−4 ± 1[d]
RDX/Al120PE10 (80:20)	0.5	180 ± 5	0.25	557 ± 17	144 ± 4	——[e]
RDX/Al120PE25 (80:20)	0.5	184 ± 5	0.26	506 ± 14	130 ± 4	——[e]
RDX/Al120PP (80:20)	0.5	165 ± 5	0.36	——[c]	——[c]	——
RDX [5]	0.2	183 ± 5	0.2	548 ± 111	139 ± 28	——[e]
RDX/Als (80:20) [5]	0.5	120 ± 10	0.4	102 ± 4	25 ± 1	−2 ± 1
RDX/Alex (80:20) [5]	0.2	172 ± 5	0.2	380 ± 138	97 ± 25	——[e]
TNT	0.4	195 ± 5	0.14	311 ± 4	75 ± 1	——[e]
TNT/Al120 (70:30)	0.5	195 ± 5	0.19	——[c]	——[c]	——
TNT/Al120PE10 (70:30)	0.5	185 ± 5	0.14	248 ± 3	60.5 ± 0.7	——[e]
TNT/Al120PP (70:30)	0.5	172 ± 5	0.13	199 ± 2	49.4 ± 0.6	——[e]
TNT [5]	0.2	220 ± 5	0.2	459 ± 18	107 ± 5	——[e]
TNT/Alex (70:30) [5]	0.3	223 ± 5	0.2	415 ± 21	97 ± 5	——[e]
TNT/Als (70:30) [5]	0.2	183 ± 9	0.2	157 ± 4	37 ± 1	——[e]
GAP	0.3	160 ± 5	0.50	149 ± 1	37.3 ± 0.2	−4 ± 1[f]
GAP/Al120 (50:50)	0.5	160 ± 5	0.42	155 ± 2	38.8 ± 0.4	−4 ± 1[f]
GAP/Al120PE10 (50:50)	0.5	154 ± 5	0.83	——[c]	——[c]	——
GAP/Al120PP (50:50)	0.5	134 ± 5	0.96	——[c]	——	——
GAP [13]	0.4	162 ± 5	0.4	197 ± 1	50 ± 1	−5 ± 1[f]
GAP [13]	0.5	154 ± 5	0.4	126 ± 2	32 ± 2	−3 ± 2[f]
GAP/Alex [13]	0.4	165 ± 5	0.7	139 ± 1	34 ± 1	−5 ± 1[f]
GAP/Als [13]	0.5	165 ± 5	0.8	132 ± 2	32 ± 1	−5 ± 1[f]
GAP/Alss [13]	0.5	143 ± 5	0.7	——[c]	——[c]	——
GAP/Alsstef [13]	0.5	130 ± 5	1.1	104 ± 1	26 ± 1	−3 ± 1[f]

[a]Onset temperature for the first detected exotherm.
[b]Pressure recorded after the system was allowed to cool to room temperature; initial pressure was 0.11 MPa.
[c]Kinetic parameters could not be estimated by regression analysis of the initial portion of the exotherm, because of the nonlinearity of the initial portion.
[d]Rate constant was calculated at 180°C.
[e]Uncertainty is larger than the value.
[f]Rate constant was calculated at 160°C.

(Table 7). There is also no significant difference in the apparent rate constant deduced from the initial part of the exotherm for thermal decomposition of RDX and RDX/Al120 (Table 7).

For the RDX/Al120PP (80:20) mixture, an onset temperature of 165°C was obtained (Table 7). This onset temperature is 20°C lower than that for neat RDX and is close to the melting point of PP, which is in the range of 160–165°C [24]. One of the possible explanations for this lower onset temperature is an interaction between the melted PP and RDX. Another possible explanation is that the bare Al nanopowder in Al120PP exposed after the melting of the PP coating lowers the RDX thermal stability. Earlier ARC results obtained for a different sample of RDX and its mixtures with Al showed that addition of Alex and Als lowered the RDX decomposition temperature by about 10 and 60°C, respectively [5]. Because the Al nanopowder used to make Al120PP had a mean particle size of 120 nm, the magnitude of its effect on the RDX decomposition is expected to be between those of Alex (180 nm) and Als (90 nm).

The bare Al nanopowder, which is exposed after the melting of the coating on Al120PP, may have a larger effect on the RDX decomposition than the uncoated Al120. Moreover, the PE coatings on Al120PE10 and Al120PE25 are expected to melt at about 90°C, and the bare Al nanopowders exposed afterward are also expected to have a similar effect to those from Al120PP. One possible explanation for this difference is the aging of Al120. Earlier DSC results have demonstrated that the reactivity of Al nanopowder depends on the aging of the material [12]. An oxide layer of 4.2 ± 0.8 nm was determined for the uncoated Al120 sample (Table 5), whereas the history of the bare Al nanopowders before the PE and PP coating process is unknown. Compared with the uncoated Al120 sample, the bare nanopowders used to produce Al120PP may have thinner oxide layers due to the lack of prior aging, thereby rendering them more reactive with RDX. Agglomeration of the nanopowders may also be a factor affecting their reactivity with RDX. The particle characterization studies have shown that Al nanopowders tend to agglomerate. The agglomerated nanopowders have smaller specific

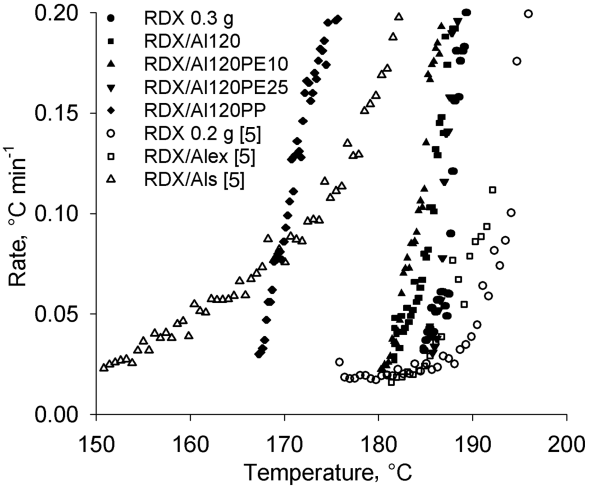

Fig. 8 Comparison of ARC results for RDX mixtures.

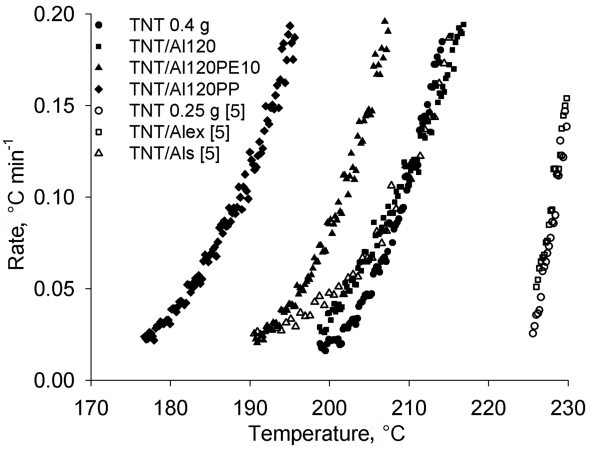

Fig. 9 Comparison of ARC results for TNT mixtures.

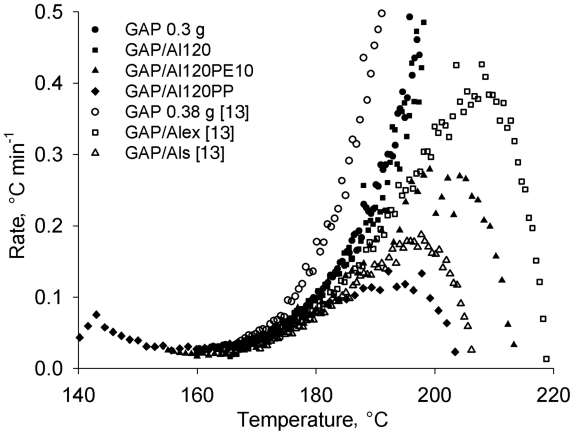

Fig. 10 Comparison of ARC results for GAP mixtures.

surface areas and are therefore expected to have a lower effect on the RDX thermal decomposition.

The ARC results show that neat TNT and the TNT/Al120 (70:30) mixture have the same onset temperature of 195°C for their thermal decomposition (Table 7 and Fig. 9). The onset temperature for TNT/Al120PE10 is slightly lower than that for TNT; however, the difference is insignificant when the uncertainty of the values is considered. With an onset temperature of 172°C, Al120PP demonstrated its effect of lowering the TNT decomposition temperature by 20°C. This effect on TNT is similar to that discussed earlier for RDX.

The ARC results show that the addition of Al120 and Al120PE10 has no effect on the onset temperature for GAP (Table 7 and Fig. 10). Al120PP lowers the GAP onset temperature by 20°C, which is also consistent with its effects on the RDX and TNT decomposition temperature. On the other hand, unlike the runaway reactions observed in RDX/Al120PP (Fig. 8) and TNT/Al120PP (Fig. 9), the exotherm observed between 140 and 200°C for GAP/Al120PP was only a minor exotherm,with a maximum self-heating rate of $\sim$0.1°C min^{-1} (Fig. 10). A similar minor exotherm was also observed for GAP/Al120PE10. Runaway reactions were only observed for these two mixtures at about 300°C during the decomposition of the coatings.

Outgassing Behavior

Chemical interaction between Al nanopowders and RDX has previously been reported [5]. In this study, the outgassing behavior of the 50:50 mixtures of RDX with the various uncoated and coated Al nanopowders at an isothermal temperature of 100°C was studied using TG-DTA-FTIR-MS. The TG-FTIR-MS results are summarized in Table 4.

Mass losses and evolutions of N_2O and H_2O were observed for neat RDX and all of the RDX/Al mixtures at 100°C. NO_2 was also detected from the RDX/Al120 mixture. Because N_2O, NO_2, and H_2O are generated from the decomposition of RDX, the evolution of these gases from the samples demonstrate a low-temperature, solid-phase decomposition of RDX.

The evolution of H_2O may also be due to the desorption of adsorbed water from the Al nanopowders. Desorption of water was reported earlier in this paper for coated and uncoated Al120 (Table 4). Compared with the uncoated sample, PE-coated Al120 showed a higher amount of adsorbed water, which also explains the higher amount of water evolved from RDX/Al120PE10 and RDX/Al120PE25 (Table 4).

An evolved gas containing [C-H] was also detected from the RDX/Al120PP mixture. The [C-H] compound may be produced from 1) the RDX decomposition, 2) the evolution of a solvent used in the PP coating process, or 3) the decomposition of the PP coating. Evolutions of HCl and HNO_3 were detected from PE-coated samples, as discussed earlier in this paper. Because these gases were not observed for RDX/Al120PE10 and RDX/Al120PE25, the newer PE-coated Al120 samples may contain lesser amounts of residues from the polymerization reaction.

Compared with that from neat RDX, a significantly higher amount of N_2O evolution was observed from all of the RDX/Al mixtures (Table 4). The TG-DTA-FTIR-MS results show that the Al nanopowders enhance the low-temperature decomposition of RDX. The same observation was obtained from the outgassing results for RDX/Als and RDX/Alex [5]. Among the various mixtures, the RDX/Al120 mixture has the highest amount of N_2O evolution. The intensities of N_2O evolution from the RDX/Al mixtures decrease as the amount of the coating increases (Table 4). The outgassing results show that the PE and PP coatings decrease the effect of Al nanopowder on the low-temperature decomposition of RDX.

ESD Sensitivities

Al nanopowders have been shown to sensitize ADN and AP to ESD [5,13]. In this study, the effects of coated and uncoated Al nanopowders on the ESD sensitiveness of ADN and AP were further studied. Table 6 summarizes the ESD results for the ADN/Al (75:25) and AP/Al (80:20) mixtures.

The ADN/Al120 and AP/Al120 mixtures ignited at a discharge energy of 6 mJ, which is substantially lower than those for neat ADN and AP. The ESD results show that addition of Al120 increases the ESD sensitiveness of ADN and AP. The effect of Al120 on the ESD sensitiveness of ADN and AP is similar to that observed for Als [5,13].

As shown in Table 6, the ESD-limiting energies obtained for the ADN and AP mixtures with Al120PE10, Al120PE25, and Al120PP are all greater than 156 mJ, as for neat ADN and AP. It can therefore be concluded that these coated Al nanopowders do not sensitize ADN and AP to the point at which precautions to prevent electrostatic charge accumulation on operators would be required to handle these mixtures.

Conclusions

The TG-DTA, DSC, and ARC results show an early oxidation of Al nanopowders below the melting point of Al. The various Al nanopowders showed significant differences in their onset temperatures, enthalpy changes, and mass gains for the solid-phase oxidation of Al. The results show that the reactivity of Al nanopowders in air depends not just on the mean particle size and the passivating layer, but also on other factors such as particle size distribution, agglomeration of powders, specific surface area, and composition of the passivating layer.

The ARC results show that all of the coated and uncoated Al nanopowders are very reactive in the presence of water, resulting in aging of the Al nanopowders. The coating of PE seems to have only a minor effect on the reactivity of Al nanopowder with water.

The aging of Al powders was further studied by exposing coated and uncoated samples of Al nanopowders to humid atmosphere at room temperature. The TG-DTA results for uncoated Al powders aged in a humid atmosphere at room temperature show a decrease in the mass gain, which implies an aging of uncoated Al powders. The coated Al nanopowders are relatively more stable than the uncoated powders in humid atmospheres.

Outgassing studies using TG-DTA-FTIR-MS show desorption of H_2O and CO_2 from Al nanopowders at 100°C. Other evolved gases, which may result from the presence of impurities, were also detected from the coated Al nanopowders. The adsorption of H_2O and CO_2 increases as the mean particle size of Al nanopowder decreases.

The results obtained for the particle characterization of Al120, Al120PE7, and Al120PE19 show that the average particle size was about 70 nm. These samples were mostly spherical single crystals, however, irregularly shaped and multicrystal particles were also observed. The Al metal core of the particle was covered by an alumina layer of $\sim$4 nm. The coating of polymer was distributed nonuniformly within clusters of nanopowders.

The ESD sensitivity measurements show that the ESD sensitivity of Al nanopowders decreases as the amount of PE coating increases.

The ARC results show that addition of Al120PP lowers the onset temperatures of RDX, TNT, and GAP by ∼20°C. No significant effect was observed from the other coated and uncoated Al nanopowders.

Outgassing studies performed on the various RDX/Al mixtures at 100°C using TG-DTA-FTIR-MS showed that the uncoated Al120 enhances the low-temperature decomposition of RDX and that the PE and PP coatings on the Al nanopowder reduce this effect.

The ESD results show that addition of Al120 increases the ESD sensitiveness of ADN and AP very significantly. This effect was not observed from the ESD results for the mixtures with Al120PE10, Al120PE25, and Al120PP. The coated Al nanopowders do not severely sensitize ADN and AP to ESD.

Acknowledgments

We would like to thank P. Brousseau of Defence Research and Development Canada—Valcartier for supporting and encouraging our research efforts in this area. Additionally, we would like to express our gratitude to C. Dubois of École Polytechnique (Université de Montréal) and H. E. Rogers and D. Hamill of Nanotechnologies, Inc., for their donations of samples. Finally, our appreciation is extended to R. Bowes of the Canadian Explosives Research Laboratory for the electrostatic discharge sensitiveness tests.

References

[1] Ivanov, G. V., and Tepper, F., edited by Kuo, K.K., *Challenges in Propellants and Combustion 100 Years After Nobel*, Begell House, New York, 1997, p. 636–645.

[2] Mench, M. M., Yeh, C. L., and Kuo, K. K., "Propellant Burning Rate Enhancement and Thermal Behaviour of Ultra-Fine Aluminum Powders (ALEX)," *Energetic Materials: Production, Processing and Characterization*, Fraunhofer-Inst. für Chemische Technologie, Pfinztal, Germany, 1998, pp. 30-1, 30-15.

[3] Lefrançois, A., and Le Gallic, C., "Expertise of Nanometric Aluminium powder on the Detonation Efficiency of Explosives," *Energetic Materials: Production, Processing and Characterization*, Fraunhofer-Inst. für Chemische Technologie, Pfinztal, Germany, 2001, pp. 36-1, 36-14.

[4] Brousseau, P., and Anderson, C. J., *Propellants, Explosives, Pyrotechnics*, Vol. 27, 2002, pp. 300–306.

[5] Kwok, Q. S. M., Fouchard, R. C., Turcotte, A.-M., Lightfoot, P. D., Bowes, R., and Jones, D. E. G., *Propellants, Explosives, Pyrotechnics*, Vol. 27, 2002, pp. 229–240.

[6] Cliff, M., Tepper, F., and Lisetsky, V., "Ageing Characteristics of Alex Nanosize Aluminium," 37th AIAA/ASME/SAE/ASEE Joint Propulsion Conference and Exhibit, AIAA Paper 2001-3287, 2001

[7] Ermoline, A., Schoenitz, M., Dreizin, E., and Yao, N., *Nanotechnology*, Vol. 13, 2002, pp. 638–643.

[8] Kwon, Y. S., Gromov, A. A., Ilyn, A. P., and Rim, G. H., *Applied Surface Science*, Vol. 211, 2003, pp. 57–67.

[9] Glebov, E. M., Yuan, L., Kishtopa, L. G., Usov, O. M., and Krasnoperov, L. N., *Industrial and Engineering Chemistry Research*, Vol. 40, 2001, pp. 4058–4068.

[10] Kimura, I., Taguchi, Y., Yoshii, H., and Tanaka, M., *Journal of Applied Polymer Science*, Vol. 81, 2001, pp. 675–683.

[11] Roy, C., Dubois, C., Lafleur, P., and Brousseau, P., "The Dispersion and Polymer Coating of Ultrafine Aluminum Powders by the Ziegler Natta Reaction," *Synthesis, Characterization, and Properties of Energetic/Reactive Nanomaterials*, Vol. 800, Materials Research Society, Warrendale, PA, 2004, pp. 79–84.

[12] Jones, D. E. G., Brousseau, P., Fouchard, R. C., Turcotte, A.-M., and Kwok, Q. S. M., *Journal of Thermal Analysis and Calorimetry*, Vol. 61, 2000, pp. 805–818.

[13] Jones, D. E. G., Turcotte, R., Fouchard, R. C., Kwok, Q. S. M., Turcotte, A.-M., and Abdel-Qader, Z., *Propellants, Explosives, Pyrotechnics*, Vol. 28, 2003, pp. 120–131.

[14] Gertsman, V. Y., and Kwok, Q. S. M., *Microscopy and Microanalysis*, Vol. 11, 2005, pp. 410–420.

[15] Kwok, Q. S. M., Emery, N., and Jones, D. E. G., *Energetic Materials (Han Neng Cai Liao)*, Vol. 13, No. 5, 2005, pp. 295–300.

[16] Dubois, C., Brousseau, P., Roy, C., and Lafleur, P., "In-Situ Polymer Grafting on Ultrafine Aluminum Powders," *Energetic Materials: Production, Processing and Characterization*, Fraunhofer-Inst. für Chemische Technologie, Pfinztal, Germany, 2004, pp. 12-1, 12-9.

[17] "Standard Practice for Heat Flow Calibration of Differential Scanning Calorimeters," American Society for Testing and Materials, Rept. ASTM E 968-02, West Conshohocken, PA, 2002.

[18] "Standard Practice for Temperature Calibration of Differential Scanning Calorimeters and Differential Thermal Analyzers," American Society for Testing and Materials, Rept. ASTM E967-03, West Conshohocken, PA, 2003.

[19] "Standard Guide for Assessing the Thermal Stability of Materials by Methods of Accelerating Rate Calorimetry," American Society for Testing Material, Rept. ASTM E1981-98R04, West Conshohocken, PA, 2004.

[20] Lightfoot, P. D., Jones, D. E. G., Fouchard, R. C., Kwok, Q. S. M., Ridley, W., and Turcotte, A.-M., "Hazard Characterization of KDNBF Using a Number of Different Techniques" *Twenty-Ninth DOD Explosives Safety Seminar Proceedings* [CD-ROM], Dept. of Defense Explosives Safety Board, Alexandria, VA, Dec. 2002.

[21] Fedoroff, B. T., and Sheffield, O. E., *Encyclopedia of Explosives and Related Items*, PATR 2700, Vol. 5, Picatinny Arsenal, Dover, NJ, 1972, pp. E-38–E-55.

[22] Johnson, C. E., Fallis, S., Chafin, A. P., Groshens, T. J., Higa, K. T., Ismail, I. M. K., and Hawkins, T. W., *Journal of Propulsion and Power*, Vol. 23, No. 4, 2007, pp. 669–682.

[23] Pesiri, D., Aumann, C. E., Bilger, L., Booth, D., Carpenter, R. D., Dye, R., O'Neill, E., Shelton, D., and Walter, K. C., "Characterization of Nanometer- to Micron-Sized Aluminum Powders: Size Distribution from Thermogravimetric Analysis," *Journal of Pyrotechnics*, Vol. 19, 2004, pp. 19–31.

[24] Lieberman, R. B., "Polypropylene (Under Olefin Polymers)," *Kirk-Othmer Encyclopedia of Chemical Technology*, 3rd ed., Vol. 16, Wiley, New York, 2002.

S. Son
Associate Editor